[Chem. Pharm. Bull. 32(10)3830—3839(1984)]

Aqueous and Nonaqueous Polarographic Studies of Substituted 2,6-Dimethylbenzonitrile *N*-Oxides[1)]

TANEKAZU KUBOTA,*,[a] SADAAKI HIRAMATSU,[a] KENJI KANO,[a] BUNJI UNO,[a] and HIROSHI MIYAZAKI[b]

Gifu Pharmaceutical University,[a] 6–1, Mitahora-higashi 5-chome, Gifu 502, Japan and Shionogi Research Laboratories, Shionogi & Co., Ltd.,[b] Fukushima-ku, Osaka 553, Japan

(Received February 8, 1984)

Aqueous and nonaqueous polarographic properties of 4-substituted 2,6-dimethylbenzonitrile *N*-oxides (stable nitrile *N*-oxides) have been studied and compared with those of the substituted pyridine *N*-oxides and benzylidenemethylamine *N*-oxides (nitrones) investigated previously by us. The first reduction wave in both the aqueous and *N*, *N*-dimethylformamide (DMF) solvent systems is due to the deoxygenation reaction of the nitrile *N*-oxide group except when certain substituents are present (see text). This conclusion has also been verified by controlled potential electrolysis in aqueous solution and by cyclic voltammetry in DMF solvent. A plot of the Hammett σ constants of the substituents against $E_{1/2}$ values was linear with a positive slope for both the aqueous and DMF solvent systems. The slope is smaller than in the case of pyridine *N*-oxides and nitrones, this being reasonably attributable to the triple bond nature of the C≡N⁼⁼O group. Half-wave reduction potentials of the nitrile *N*-oxides are positively shifted compared with those of pyridine *N*-oxides, particularly in an aqueous solvent. Molecular orbital calculations were applied to interpret the substituent effect on the reduction potentials of the *N*-oxides.

Keywords——aqueous polarography; nonaqueous polarography; substituent effect on half-wave potential; cyclic voltammetry; controlled potential electrolysis; PPP-SCFMO; CNDO/2; LUMO energy; 4-substituted 2,6-dimethylbenzonitrile *N*-oxide

The chemistry of aromatic tertiary amine *N*-oxides was extensively developed by Ochiai and his colleagues,[2)] and the characteristic nature of the *N*-oxide bond was discussed in detail in Ochiai's book.[2)] In the previous papers[3–9)] one (T. K.) of the present authors described a new type of tertiary amine *N*-oxides theoretically and experimentally, a typical example of which is benzonitrile *N*-oxide (shown in Fig. 1). As can be understood from Fig. 1, the N–O bond has a triple bond nature, since the C≡N→O group is in a linear configuration, *i.e.*, the carbon and nitrogen atoms in the C≡N bond are in *sp*-hybridization. This was verified by X-ray crystallographic analyses,[6,9)] infrared (IR) and ultraviolet (UV) spectra,[4,7)] the basicity of the *N*-oxide group oxygen atom, *etc.*[3,5,8)] The N–O bond distance and the N–O stretching

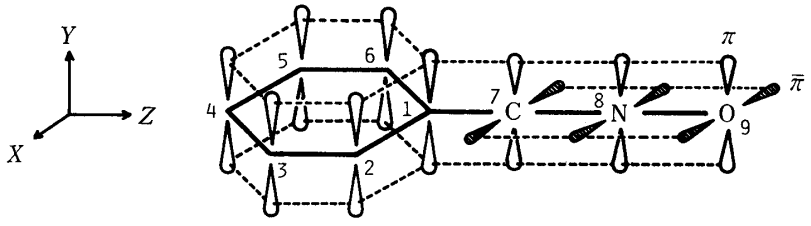

Fig. 1. Schematic Illustration of π and $\bar{\pi}$ Type Resonance Systems of Benzonitrile *N*-Oxide

The MO calculation was performed by using the numbering and the coordinate axes given in this figure.

band are shorter and at higher frequency, respectively, than those of other kinds of *N*-oxide bonds. In this work, aqueous and nonaqueous polarographic studies have been carried out on substituted benzonitrile *N*-oxides. The results are discussed and compared with our previous polarographic data on substituted pyridine *N*-oxides and benzylidenemethylamine *N*-oxides (nitrones),[10-12] in which the N–O bond has double bond character.

Experimental

Polarographic Measurements——The instruments and the techniques used for the measurements of aqueous and nonaqueous direct current (DC) polarograms and cyclic voltammograms (CV) were the same as described in detail in the foregoing papers.[13,14] Alternating current (AC) polarographic measurements were performed by fitting an auto-lock-in amplifier NF LI-572B and a functional generator NF FG-121B (an AC signal generator) to the above polarographic instruments. Capillary constants employed for the mercury drop electrode were as follows: $h=80$ cm, $m=2.672\,\mathrm{mg\,s^{-1}}$, $t=3.88$ s in distilled water at open circuit. In the case of aqueous solutions, all the measurements were carried out in a mixed solution composed of 70% (v/v) buffer solution and 30% (v/v) ethanol because of sample solubility considerations. The systems of buffer solutions are: HCl + NaAc for pH = 1.00—5.20; $KH_2PO_4 + Na_2HPO_4$ for pH = 5.91—8.04; $NaOH + KH_2PO_4$ for pH = 6.2—7.6; NaOH + glycine for pH = 8.24—12.10. The pH values of the final buffer solutions containing ethanol were measured with a glass electrode.[15] The ionic strength of all the buffer solutions was controlled to 0.5 by the addition of NaCl. In addition, a small amount of gelatin was added to the sample solution as a maximum wave suppressor, since a maximum wave or a trough-shaped wave appeared, especially in the pH region less than *ca* 4, the most suitable concentration being 0.005%. All the voltammetric measurements were made at 25 ± 0.1 °C and against a saturated calomel electrode (SCE), unless otherwise noted, after bubbling nitrogen or argon gas through the solution to remove the dissolved oxygen. The nonaqueous voltammograms were recorded in *N*,*N*-dimethylformamide (DMF) containing 0.1 mol dm^{-3} tetrapropylammonium perchlorate (TPAP). DMF was dried over molecular sieves (Wako Pure Chemical Molecular Sieves 5A 1/16), then carefully distilled under reduced pressure in a nitrogen atmosphere. TPAP was purified as described in earlier papers.[16,17]

Controlled Potential Electrolysis——This electrolysis was carried out using a Yanagimoto controlled potential electrolyzer, model VE-10. The quantity of electricity was measured by the use of a copper coulometer[18] as well as by graphic integration of the current-time curve. The current due to the electrolytic solution with no sample was then subtracted from the overall value as being a base current due solely to the buffer or TPAP component. Figure 2 shows the electrolysis cell used here, which was designed for both aqueous and nonaqueous electrolysis.

Samples——The substances used were 4-substituted 2,6-dimethylbenzonitrile *N*-oxides (see Fig. 3 for molecular dimensions), as listed in Table I. In general, benzonitrile *N*-oxides are unstable and easily dimerized to furoxans at room temperature, but their 2,6-dimethyl derivatives are stable even at room temperature and are known as stable nitrile *N*-oxides.[19] All of these stable nitrile *N*-oxides (see Table I) were prepared by Grundmann's method, *i.e.*, by

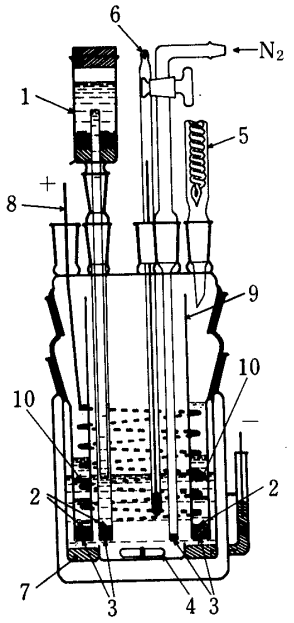

Fig. 2. Controlled-Potential Electrolysis Cell Designed for Aqueous and Nonaqueous Experiments

(1) SCE. (2) Salt Bridge.[12] (3) Fine and coarse (only for N_2 gas inlet tube) glass filters. (4) Magnetic stirrer. (5) Cooler position, if necessary. (6) Thermometer. (7) Mercury cathode. (8) Pt anode. (9) Separator tube, the outside and the inside of which are used for cathode and anode solutions, respectively. (10) Large holes made in the separator tube 9. The separator tube has three such holes which permit efficient circulation of the cathode solution. However, the flanges of the holes were tightly fixed to the separator tube, so that the cathode solution could not mix with the anode solution inside the separator tube. The current passes through the fine sintered glass filter set in the bottom of the separator tube 9.

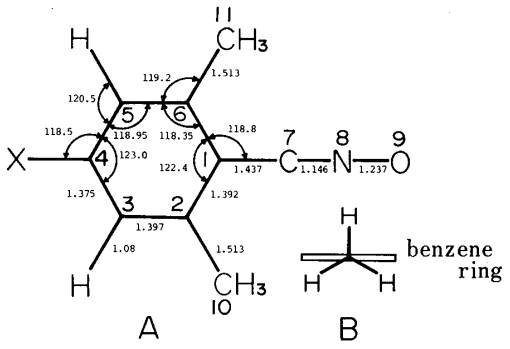

Fig. 3

(A): molecular dimensions of 4-substituted 2,6-dimethylbenzonitrile *N*-oxides employed for PPP and CNDO/2 calculations. (B): methyl configuration adopted for CNDO/2 calculation. See the text for details.

TABLE I. 4-Substituted 2,6-Dimethylbenzonitrile *N*-Oxides and the Corresponding Nitriles Investigated, with Their Melting Points, First ($E_{1/2\cdot1}$) and Second ($E_{1/2\cdot2}$) Reduction Potentials in Aqueous and DMF Solvent Systems, and LUMO Energies Calculated by CNDO/2 and PPP Methods

Substituent	Nitrile *N*-oxides						Corresponding nitriles	
	mp (°C)	$E_{1/2\cdot1}$ (V)[a]		$E_{1/2\cdot2}$ (V)[a]	LUMO (eV)		mp (°C)	$E_{1/2\cdot1}$ (V)[a]
		H_2O	DMF[b]	DMF[b]	CNDO/2	PPP		DMF[b]
H	81	−0.304	−1.985	−2.397	2.378	−2.144	86—88	−2.400
CH_3	109—110	−0.293	−2.074	−2.505	2.381	−2.099	50	−2.477
Cl	111—112	−0.253	−1.725	−2.415	1.664	−2.110	59—60	−1.970 (−2.405)[c]
Br	97—98.5	−0.243	−1.827	−2.405	—	—	68—70	−1.915 (−2.395)[c]
OCH_3	68—71	−0.324	−2.150	−2.600	2.584	−2.056	71—72	−2.600
$N(CH_3)_2$	134	−0.398	−2.300	−2.730	2.670	−1.626	89—91	−2.730
CN	129 (dec.)	−0.210	−1.500	−1.635	1.701	−2.555	165—167	−1.645
NO_2	131—132	−0.177	−0.925	−1.405	0.898	−3.648	122—123	−0.880

a) Reduction potentials *vs.* SCE are listed in this table.
b) DMF means *N*, *N*-dimethylformamide.
c) The values in parentheses are for the reduction potentials appearing as $E_{1/2\cdot2}$ and are due to the dehalogenated nitriles.

the reaction of the corresponding aldoxime with NaOBr at a low temperature,[20] and then recrystallized several times from ether except in the case of the $N(CH_3)_2$ substituent; recrystallization of the latter product was done from methanol. The aldoximes mentioned above were prepared by the reaction of hydroxylamine with the corresponding aldehydes, which were synthesized by the cited methods: for X=H, Cl, Br, CN and NO_2 in Fig. 3, the Beech reaction;[21] for X=OCH_3, the Adams modification[22,23] of the Gattermann reaction; and for X=$N(CH_3)_2$, the Vilsmeier–Haack reaction.[24,25] 2,4,6-Trimethylbenzaldehyde was purchased from Aldrich Chemicals. The nitriles (4-substituted 2,6-dimethylbenzonitriles) corresponding to Fig. 3, which were required to identify the nonaqueous polarograms of 4-substituted benzonitrile *N*-oxides, were easily obtained by any one of the following methods: by deoxygenation from the nitrile *N*-oxides with $(C_2H_5O)_3P$[26] for X=H, CH_3, Cl, OCH_3, CN and NO_2; by dehydration of the oxime with acetic anhydride for X=$N(CH_3)_2$;[27] and by the reaction of the diazonium salt of 4-bromo-2,6-xylidine with $CuSO_4$ and NaCN for X=Br.[28] The purity of all the compounds was carefully checked by elemental analysis and spectroscopic methods (UV, IR *etc.*).

Molecular Orbital Calculation——In order to interpret the nature of the nonaqueous half-wave reduction potentials of benzonitrile *N*-oxides, molecular orbital calculations were done by using the methods of Pariser-Paar-Pople (PPP) and the model 2 type of complete neglect of differential overlap (CNDO/2).[13,14] In the case of PPP calculation, the parameters such as core-resonance integral $\beta_{\mu\nu}^{core}$, valence state ionization potential I_p, electron affinity E_A, bond length and bond angle pertaining to the substituents, *etc.* are the same as reported in the foregoing papers.[13,29] The molecular dimensions of benzonitrile *N*-oxides were derived from the X-ray crystallographic analysis data for 2,4,6-trimethylbenzonitrile *N*-oxides, *etc.*,[9] the skeletons of which deviate slightly from C_{2v} symmetry because of the intermolecular interactions in the crysrals. However, to keep the C_{2v} symmetry for convenience' sake we modified the X-ray dimensions a little as follows: the angles $\angle 123 = \angle 165 = 118.35°$ (mean value), $\angle 234 = \angle 654 = 118.95°$ (mean value), and the atoms 7, 8 and 9 are put on the C_2 axis, as shown in Fig. 3. The

other details are also given in Fig. 3. The values of C(sp^2)–H = 1.08 Å and C(sp^3)–H = 1.09 Å were assumed for C–H bond length.[13] The CH_3 configuration was put as in Fig. 3-B for CNDO/2 calculation, since CH_3 hyperconjugation with benzene ring π electrons is most favorable.[30] It should be noted that the CH_3 groups at the 2 and 6 positions do not cause any steric hindrance to the C≡N→O group, since it is in a linear configuration.[4,6,7,9]

Results and Discussion

Aqueous Polarographic Behavior of Benzonitrile *N*-Oxides

All the benzonitrile *N*-oxides listed in Table I are easily reduced at the dropping mercury electrode, and the half-wave reduction potential $E_{1/2}$ values are pH-dependent. As a typical example, the polarogram of the *p*-CH_3 derivative is depicted in Fig. 4, where we see that the maximum type second wave appears in acidic solutions. The current decreases rapidly with increasing pH and disappears at about pH 4. On the other hand, in the pH region above about 8 the first reduction wave decreases in current and vanishes at about pH 10. This kind of behavior of the reduction waves was seen for all the nitrile *N*-oxides employed here. The pH dependence of the above reduction waves and $E_{1/2}$ values is shown in Fig. 5 for the *p*-CH_3 substituent, as a typical example. The origin of the maximum type second wave is not clear at present, but it might be the catalytic hydrogen wave caused by benzonitrile *N*-oxides in acidic media.[31] The decrease of the first wave-height in the alkaline region is clearly brought about by the decomposition of the *N*-oxides; this was confirmed by UV spectroscopic investigation under almost the same experimental conditions as those of the polarographic measurements (see curves 4a, 4b in Fig. 5). The plot of $E_{1/2}$ *vs.* pH is linear with a slope of −62.44 mV for the *p*-CH_3 substituent in the pH region from 4 to 7, as shown in Fig. 5. This linearity, however, is not maintained in the pH region below about 4 or above about 7, where other straight lines with smaller slopes are apparent (Fig. 4). It is of interest to note that the crossing points of the lines located at about pH 4 or 7 are in the pH regions where the above-mentioned second

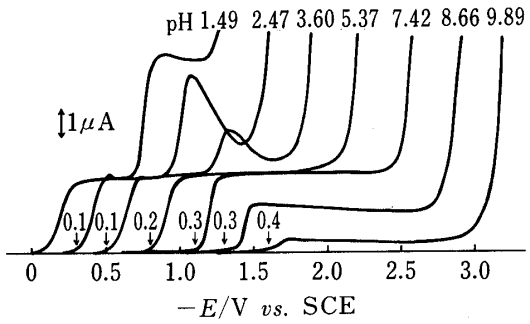

Fig. 4. The pH Dependence of the Polarogram of 2,4,6-Trimethylbenzonitrile *N*-Oxide

The abscissa scale is given for the curve at pH 1.49. The scales for other polarograms are negatively shifted to avoid complexity in the figure, and are indicated by arrows for the set potential of each polarogram.

Buffer, ethanol = 30 v/v%; μ = 0.5; gelatin = 0.005%; conc. = 5.0417×10^{-4} mol dm^{-3}.

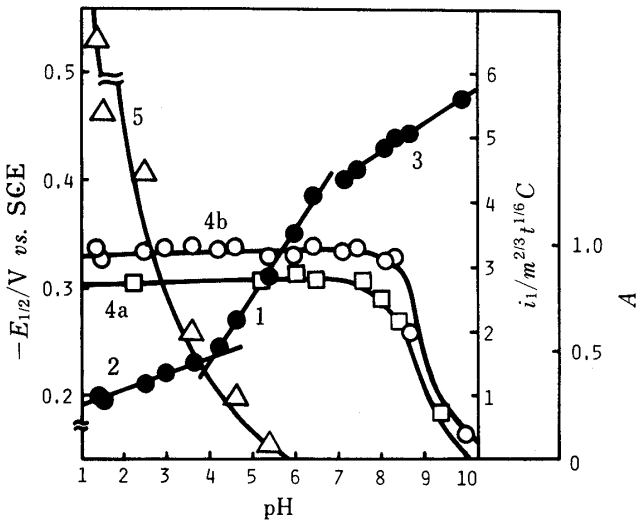

Fig. 5. Behavior of the Reduction Waves and Potentials as well as the UV Intensity of 2,4,6-Trimethylbenzonitrile *N*-Oxide with Change of pH

(1, 2, 3) linear pH dependence of the first reduction potential; (4a) pH dependence of the 260 nm maximum absorbance; (4b) pH dependence of the first reduction wave-hight expressed in terms of the Lingane constant; (5) pH dependence of the second reduction wave-height appearing in the acidic region. See the right ordinate scale for Lingane's constant and absorbance (*A*).

reduction wave in the acidic region almost disappears or the decomposition of the sample in the alkaline region just begins, respectively. Hereafter we employ the $E_{1/2}$ values in the pH region from 4 to 7 for discussion. The slopes of the $E_{1/2}$ *vs.* pH plot in this pH region are −50.76, −62.44, −53.90, −63.93, −58.40, and −58.70 in mV unit for X (see Fig. 3)=H, CH_3, Cl, Br, OCH_3, and $N(CH_3)_2$, respectively, and are close to the values found in the cases of nitrones[11] and pyridine *N*-oxides.[10]

Nonaqueous Polarographic Behavior of Benzonitrile *N*-Oxides

Figure 6 shows the DC and AC reduction polarograms and CV curve in DMF solvent for 2,4,6-trimethylbenzonitrile *N*-oxide (a typical example), these results being comparable with those obtained in an aqueous system.

All the nonaqueous polarographic reduction potentials of nitrile *N*-oxides and the corresponding nitriles studied here are listed in Table I. Although the anion radical is generally formed at the nonaqueous first reduction wave of usual aromatic substances, including heterocyclic amine *N*-oxides, the DC, AC, and CV curves shown in Fig. 6 clearly indicate an irreversible process. The nitrile *N*-oxides presumably undergo electrochemical reduction at the first wave. In addition, the second half-wave reduction potential, $E_{1/2\cdot 2}$, of the *N*-oxides agrees well with the first reduction potential of the corresponding nitriles (see Table I), and the reduction waves corresponding to the $E_{1/2\cdot 2}$ values of the *N*-oxides and those pertinent to the first reduction potentials of the nitriles correspond to a good reversible redox system as is apparent from the AC and CV curves in Fig. 6, where we see that for the case of the reduction wave due to the reversible redox system wave-height of the AC curve is quite high and the anodic wave on the reverse scan is clearly seen in the CV curve. These results can be explained in terms of the anion radical formation of the corresponding nitriles produced at the first reduction wave of the nitrile *N*-oxides employed.[32,33] For the case of 2,6-dimethyl-4-nitrobenzonitrile *N*-oxide, however, the measurements of the CV and AC curves indicated that the anion radical formation occurs at the first wave of the nitrile *N*-oxide. Further, the nonaqueous polarograms for the compounds with 4-Br and 4-Cl substituents indicated that the pattern and the wave-height of the first reduction wave are quite different from and rather larger than those of the other *N*-oxides. In addition, the wave-height and the reduction potential of the second wave and the corresponding CV curve with the above halogen

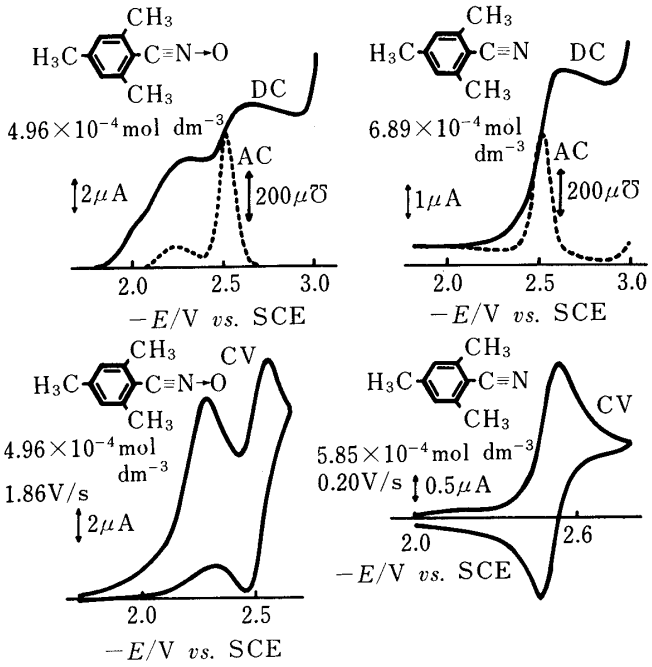

Fig. 6. Nonaqueous DC and AC Polarograms and Cyclic Voltammograms in DMF of the Compounds Given in the Figure

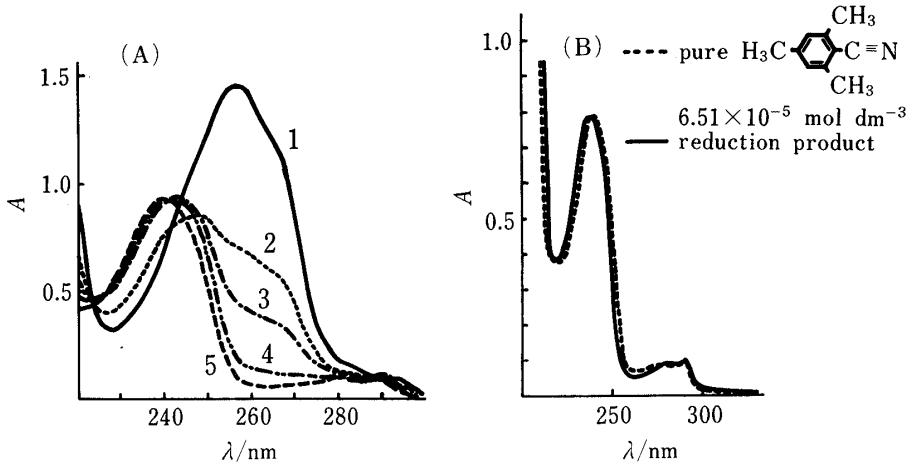

Fig. 7. (A) The Change of the UV Spectrum of 2,4,6-Trimethylbenzonitrile *N*-Oxide with the Lapse of Time during Controlled-Potential Electrolysis

Curve 1 is for the *N*-oxide before electrolysis; curves 2, 3, 4, and 5 are the spectra after electrolysis for 1 h, 2 h, 4 h, and 6 h, respectively.

(B) Comparison of the UV Spectra of Pure 2,4,6-Trimethylbenzonitrile and the Reduction Product Obtained Here

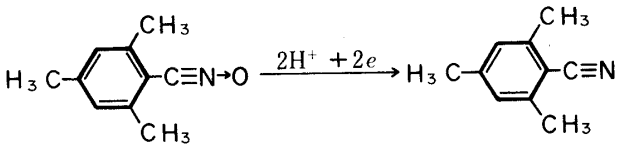

Chart 1

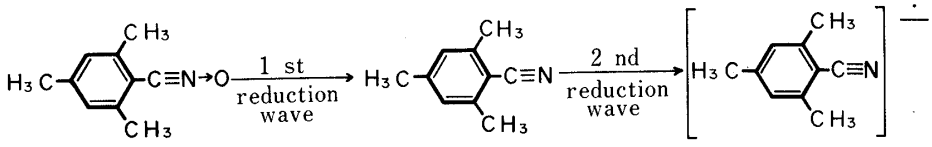

Chart 2

substituents are in good agreement with the first wave of 2,6-dimethylbenzonitrile, indicating that the dehalogenation[34] and the deoxygenation reactions occur at the first reduction wave of the halogen-substituted nitrile *N*-oxides.

Reduction Mechanism of the Benzonitrile *N*-Oxides in Aqueous and Nonaqueous Media

In order to elucidate the reduction mechanism, we firstly carried out a controlled-potential electrolysis of 2,4,6-trimethylbenzonitrile *N*-oxide under conditions similar to those of the polarographic measurements. The sample solution of 2.86×10^{-3} mol dm^{-3} in buffer solution containing 45% (v/v) ethanol was electrolyzed under a nitrogen atmosphere at -0.70 V and constant apparent pH = 5.93. The time course of the electrolysis was followed by UV spectral measurement, the result being illustrated in Fig. 7A, in which we see that the strong absorption band at about 260 nm characteristic of the *N*-oxide decreases in intensity with the lapse of time, and almost completely disappears after 4 h. The electrolyzed product was extracted with benzene and chloroform. The extract was washed with water, dried with Na_2SO_4, then evaporated. The residue was sublimed under reduced pressure. The mp (49 °C) and UV and IR spectra of the compound thus obtained are consistent with those of the corresponding nitrile (2,4,6-trimethylbenzonitrile). Figure 7B compares the above UV spectra. These experimental results can be ascribed to the two-electron reduction ($n = 2$) of the

N-oxide as shown in Chart 1. The above controlled-potential electrolysis gave an average *n* value (calculated from the quantities of electricity obtained by the Cu-coulometer and graphic integration) of 1.71 at pH 5.93.[35a,b] Alternatively the *n* value calculated from the Ilkovic equation using the diffusion constant $D=6.2\times10^{-6}$ cm^2 s^{-1} for the *N*-oxide (estimated by use of the Stokes–Einstein equation[36]) is 1.8—1.9 at pH 5.40.[35]

As mentioned above, the reduction mechanism of the nitrile *N*-oxides in nonaqueous solvents can be expressed as in Chart 2, except for the 4-nitro substituted compound, the anion radical of which is produced at the first wave, and for the 4-Cl and 4-Br substituted compounds, where dehalogenation as well as deoxygenation occurs at the first wave.

Substituent Effect on the Reduction Potentials

As we have discussed in previous papers, the half-wave reduction potentials should be linearly correlated with the Hammett-type substituent constants such as σ_p *etc.*, if the potential-determining step is mainly controlled by the same mechanism in a series of substances tested.[37] Line 3 in Fig. 8 is the $E_{1/2}$ *vs.* σ plot for 4-substituted benzonitrile *N*-oxides, where the potentials are those at pH = 5.0 (see Table I). The linearity seems to be very good, and the reduction potentials should correspond to the deoxygenation step (see Chart 1) for all substituents.[38] This conclusion is the same as for pyridine *N*-oxides and nitrones reported in our previous papers.[10-12] The $E_{1/2}$ *vs.* σ plots for pyridine *N*-oxides and nitrones are reproduced in Fig. 8 for comparison with that of benzonitrile *N*-oxides. We can now easily understand that the benzonitrile *N*-oxides are polarographically much more easily reduced than pyridine *N*-oxides and benzylidenemethylamine *N*-oxides (nitrones), and, fall in the reduction potential region of the aromatic nitro group, which is polarographically very active. This seems to be a characteristic property of aromatic nitrile *N*-oxides. Now let us consider the slope of the straight line 3, corresponding to benzonitrile *N*-oxides, shown in Fig. 8. The

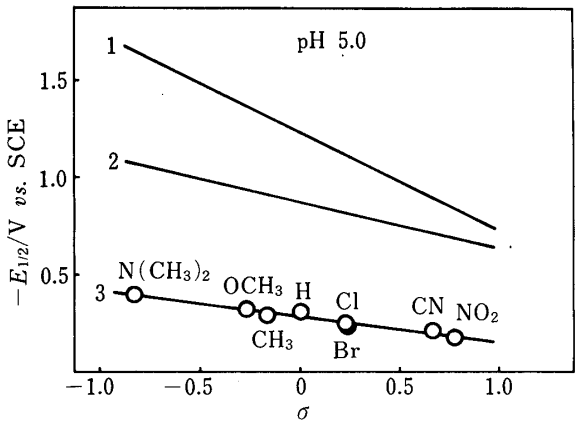

Fig. 8. Linear Relation (Line 3) between Aqueous Half-Wave Reduction Potentials at pH 5.0 and σ_p Constants for 4-Substituted 2,6-Dimethylbenzonitrile *N*-Oxides

The solid lines 1 and 2 are for the substituted aromatic *N*-oxides (1) and (2) shown below, respectively, taken from our previous work.[10-12] The least-squares equations are: $E_{1/2}=0.504\sigma-1.23$ ($r=0.9702$), $E_{1/2}=0.237\sigma-0.872$ ($r=0.9685$), $E_{1/2}=0.133\sigma-0.286$ ($r=0.9866$) for lines 1, 2 and 3, respectively. Here *r* denotes the Pearson correlation coefficient.

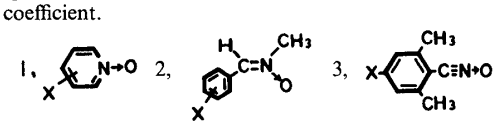

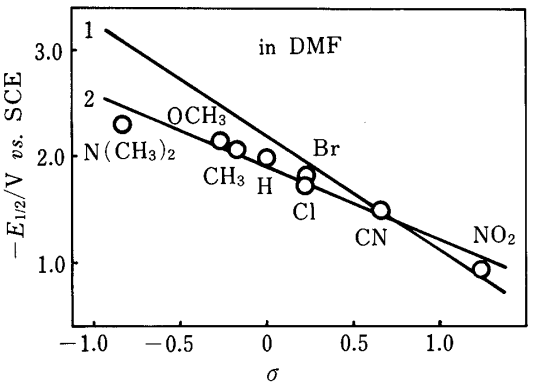

Fig. 9. Linear Relation (Line 2) between Nonaqueous Half-Wave Reduction Potentials in DMF and σ_p Constants for 4-Substituted 2,6-Dimethylbenzonitrile *N*-Oxides

The solid line 1 is for the substituted pyridine *N*-oxides already reported by us.[12] The least-squares equations are: $E_{1/2}=1.068\sigma-2.202$ ($r=0.9896$) and $E_{1/2}=0.684\sigma-1.904$ ($r=0.9738$) for lines 1 and 2, respectively. Here *r* is the Pearson correlation coefficient.

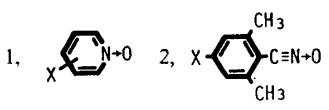

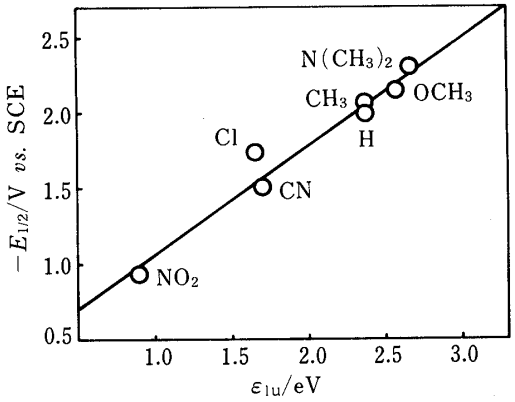

Fig. 10. Correlation of Nonaqueous Half-Wave Reduction Potentials and CNDO/2 LUMO Energies for 4-Substituted 2,6-Dimethylbenzonitrile *N*-Oxides

The least-squares equation is $E_{1/2} = -0.721\varepsilon_{1u} - 0.338$ with $r = 0.9806$.

slope is clearly smaller than those of the other two kinds of aromatic *N*-oxides, and a similar tendency is apparent in Fig. 9 (discussed later). This means that the electronic nature of the C≡N→O group is not so sensitive to the substitution of an electron donor or acceptor. The main reason is presumably as follows. As shown in Fig. 1, the N–O group in benzonitrile *N*-oxides exhibits a triple bond nature, so that the N–O bond order becomes quite large. Spectroscopic and intermolecular interaction experiments support this consideration.[3-9] In addition, the polar N–O bond seems to be largely hydrated in an aqueous medium.[39,40] Further, the methyl groups at the 2 and 6 positions are able to bring about a hyperconjugation effect on the benzene ring. These circumstances are unfavorable to a strong substituent effect on the C≡N→O group in benzonitrile *N*-oxides.

The $E_{1/2}$ *vs.* σ plot for the data obtained in DMF is shown in Fig. 9, in which our previous results on the substituted pyridine *N*-oxides are included for comparison.[12] The fact that all the $E_{1/2}$ values fall on a good straight line indicates that the potential-controlling step in the nonaqueous reduction process may be the same for all the compounds, and the electron transfer process from the mercury electrode to samples should play an important role. The half-wave potentials obtained in DMF are very negatively shifted in comparison with the data in the aqueous medium (see also Table I and Fig. 8). This can be ascribed to the difference of solute-solvent interaction of the *N*-oxides (*vide ante*). The slope of the linear relation in Fig. 9 indicates that the $E_{1/2}$ *vs.* σ slope of the substituted benzonitrile *N*-oxides is smaller than in the case of pyridine *N*-oxides as has been observed in Fig. 8. One of the reasons is presumably the triple bond nature of the C≡N→O group (*vide ante*). Finally, we will discuss the relation of nonaqueous half-wave reduction potentials to the lowest unoccupied molecular orbital (LUMO) energies, since it is well known that the potentials are intimately related to the LUMO energies.[10,13,14,41] Figure 10 shows the relation between the CNDO/2 LUMO energies and the nonaqueous $E_{1/2}$ values for a series of benzonitrile *N*-oxides. The correlation coefficient is 0.9806 and seems to be quite good, as is theoretically expected.[42] These results again suggest that the potential-determining step is mainly governed by the electron transfer process from the mercury electrode to the LUMO orbital. Keeping in mind the fact that the above $E_{1/2}$ values are in a linear relation to the substituent constant σ, we can predict that the LUMO energy (E) *vs.* σ plot should also be linear. The results are as follows: for the equation $\varepsilon_{1u} = a\sigma + b$, $a = -0.905$, $b = 2.151$ with $n = 7$, $r = 0.9451$, $s = 0.2303$ in the case of CNDO/2 calculation, but $a = -0.900$, $b = -2.209$ with $n = 7$, $r = 0.9382$, $s = 0.2445$ in the PPP calculation. These results seem to be consistent with the above considerations.

References and Notes

1) Presented at the 103rd (Tokyo, April 1983) Annual Meeting of the Pharmaceutical Society of Japan (Abstract,

p. 545), and the 29th Symposium of Polarography and Electrochemical Analysis (Nagaoka, October 1983) (Abstract, *Rev. Polarogr. (Kyoto)*, **29**, 91 (1983)).
2) E. Ochiai, "Aromatic Amine Oxides," Elsevier, Amsterdam, 1967.
3) T. Kubota, M. Yamakawa, M. Takasuka, K. Iwatani, H. Akazawa, and I. Tanaka, *J. Phys. Chem.*, **71**, 3597 (1967).
4) M. Yamakawa, T. Kubota, and H. Akazawa, *Bull. Chem. Soc. Jpn.*, **40**, 1600 (1967).
5) T. Kubota, K. Ezumi, M. Yamakawa, and Y. Matsui, *J. Mol. Spectrosc.*, **24**, 378 (1967).
6) M. Shiro, M. Yamakawa, and T. Kubota, *Chem. Commun.*, **1968**, 1409.
7) M. Yamakawa, T. Kubota, H. Akazawa, and I. Tanaka, *Bull. Chem. Soc. Jpn.*, **41**, 1046 (1968).
8) J. Bastide, J. P. Maier, and T. Kubota, *J. Electron Spectrosc. Relat. Phenom.*, **9**, 307 (1976).
9) M. Shiro, M. Yamakawa, and T. Kubota, *Acta Cryst.*, **B35**, 712 (1979).
10) T. Kubota and H. Miyazaki, *Bull. Chem. Soc. Jpn.*, **39**, 2057 (1966).
11) T. Kubota, H. Miyazaki, and Y. Mori, *Bull. Chem. Soc. Jpn.*, **40**, 245 (1967).
12) T. Kubota, K. Nishikida, H. Miyazaki, K. Iwatani, and Y. Ōishi, *J. Am. Chem. Soc.*, **90**, 5080 (1968).
13) T. Kubota, B. Uno, Y. Matsuhisa, H. Miyazaki, and K. Kano, *Chem. Pharm. Bull.*, **31**, 373 (1983).
14) B. Uno, Y. Matsuhisa, K. Kano, and T. Kubota, *Chem. Pharm. Bull.*, **32**, 1 (1984).
15) Strictly speaking, these pH values are apparent ones for aqueous solutions containing ethanol.
16) D. H. Geske and A. H. Maki, *J. Am. Chem. Soc.*, **82**, 2671 (1960).
17) H. Miyazaki, T. Kubota, and M. Yamakawa, *Bull. Chem. Soc. Jpn.*, **45**, 780 (1972).
18) D. Dobos, "Electrochemical Data—A Handbook for Electrochemists in Industry and Universities," Elsevier, Amsterdam, 1975, p. 285.
19) Note that the CH_3 groups at the 2 and 6 positions never have a steric effect on the $C\equiv N\rightarrow O$ group.[4] However the CH_3 groups can sterically prevent the reaction of the $C\equiv N\rightarrow O$ group with other molecules (reagents, *etc.*).
20) Ch. Grundmann and P. Grünanger, "The Nitrile Oxides—Versatile Tools of Theoretical and Preparative Chemistry," Springer-Verlag, Berlin, Heidelberg, New York, 1971.
21) W. F. Beech, *J. Chem. Soc.*, **1954**, 1297.
22) R. Adams and I. Levine, *J. Am. Chem. Soc.*, **45**, 2373 (1923).
23) R. Adams and E. Montgomery, *J. Am. Chem. Soc.*, **46**, 1518 (1924).
24) E. Campaigne and W. L. Archer, "Organic Syntheses," Coll. Vol. IV, John Wiley and Sons, Inc., New York, 1963, p. 331.
25) C. Grundmann and J. M. Dean, *Angew. Chem.*, **77**, 966 (1965).
26) C. Grundmann and H-D. Frommeld, *J. Org. Chem.*, **30**, 2077 (1965).
27) Private communication from Dr. H. Akazawa, Shionogi Research Laboratories, Shionogi & Co., Ltd.
28) H. T. Clarke and R. R. Read, "Organic Syntheses," Coll. Vol. I, John Wiley and Sons, Inc., New York, 1941, p. 514.
29) The hyperconjugation effect due to methyl groups is taken into account in the PPP calculation by decreasing the I_p of the atom bonded to the methyl group by 0.5 eV. See references 37 and 41 cited in ref. 13 of the present paper.
30) K. Higashi and H. Baba, "Quantum Organic Chemistry," (in Japanese), Asakura Publishing Company, Tokyo, 1956, p. 176.
31) For the case of heterocyclic amine *N*-oxides such as pyridine *N*-oxide, *etc.*, this kind of maximum wave could not be recorded even in the acidic region.
32) These results are in accord with previous ESR study.[33]
33) H. Miyazaki, K. Nishikida, and T. Kubota, *Bull. Chem. Soc. Jpn.*, **44**, 277 (1971).
34) This kind of dehalogenation reaction also occurs frequently in other types of aromatics.[13]
35) *a*) Both the n and D values have been determined at the same time by means of potential-step chronoamperometry at pH 5.00,[35b] values of $n=1.96$ and $D=3.78\times10^{-6}\,cm^2\,s^{-1}$ being obtained. This D value, however, seems to be a little smaller than those of the other similar substances. When we apply this D value to the Ilkovic equation the n value becomes a little larger than 2. In the case of controlled potential electrolysis, there might be some side reaction in the course of the electrolysis, so that the n value is apparently reduced to 1.71. *b*) H. Ikeuchi, Y. Fujita (née Aihara), K. Iwai, and G. P. Sato, *Bull. Chem. Soc. Jpn.*, **49**, 1883 (1976).
36) I. M. Kolthoff and J. J. Lingane, "Polarography," 2nd ed., Vol. I, Interscience, New York, 1952, p. 56.
37) P. Zuman, "Substituent Effect in Organic Polarography," Plenum Press, New York, 1967, See also ref. 13 and other papers cited therein.
38) The aqueous polarogram of the 4-nitro substituted compound shows two reduction waves, *i.e.*, the first ($E_{1/2\cdot1}$) and the second ($E_{1/2\cdot2}$) reduction potentials at pH = 5.0 are 0.177 and 0.294 V, respectively. The wave-height of the latter is about 1.7 times larger than that of the former. The above $E_{1/2\cdot2}$ value accords well with the reduction potential (−0.289 V at pH = 5.0) of 4-nitro-2,6-dimethylbenzonitrile, which is produced at the potential $E_{1/2\cdot1}$. Thus, the $E_{1/2\cdot1}$ value was used for plotting on line 3 in Fig. 8, and falls quite well on the straight line. The $E_{1/2\cdot2}$ value is assigned to the reduction of the 4-nitro group.

39) The substituent constant of the NO_2 group best fitting line 3 in Fig. 8 was the usual σ_p value in lieu of σ^-, which was the best for the nonaqueous solvent data given in Fig. 8. This result supports the idea that the two-way intramolecular charge-transfer ability of the *N*-oxide group[40] is reduced in an aqueous solvent because of the hydration effect.
40) R. S. Mulliken and W. B. Person, "Molecular Complexes," Wiley-Interscience, New York, 1969, pp. 287, 292.
41) B. Uno, Y. Matsuhisa, K. Kano, and T. Kubota, *Chem. Pharm. Bull.*, **32**, 1691 (1984) and other papers cited therein.
42) For PPP LUMO energies this kind of correlation gives $n=7$, $r=0.9559$, and $s=0.1523$.